Journal of
Renewable Energy Research and Applications (RERA)

Published online

Enhanced power extraction by splitting a single flap-type wave energy converter into a double configuration

A. Abazari[1*] and M.M. Aziminia[2*]

1. Chabahar Maritime University, Chabahar, Iran.
2. School of Mechanical Engineering, Sharif University of Technology, Tehran, Iran.

Received Date 20 April 2022; Revised Date 06 May 2022; Accepted Date 08 June 2022
**Corresponding author: abuzarabazari@cmu.ac.ir (A. Abazari)*

Abstract
Flap-type wave energy converter is one of the oscillating surge devices for generating electricity from the ocean wave source. It comprises a vertical plate pivoted on a hinged base that oscillates rotationally due to the exciting wave. Splitting a single flap into two separated flaps in a double arrangement may cause different dynamic characteristics. This can improve the output extracted power versus the excitation period. Therefore, this effect is investigated in the present work through a dynamic mathematical model. The hydrodynamic coefficients and exciting torques in the equation are calculated based on the boundary element-based software of ANSYS AQWA. In the next step, the rotational displacement is calculated through the frequency domain approach based on the assumption of the regular monochromatic and head-on waves, and consequently, the maximum power is computed regarding the optimum power take-off damping strategy. Finally, in the same procedure as the single flap, the output power for the double arrangement is derived. The results obtained show that decreasing the natural period for each flap can potentially cause a wideband response of the total power for the double configuration compared to the single one.

Keywords: *Water wave, oscillating wave surge converter, frequency domain analysis, single and double flap.*

1. Introduction

Global warming is a great issue threatening our planet. A key solution to overcome the climate change is to harness renewable energy resources. Ocean waves are one of the planet's most reliable and promising renewable energy sources, as the wind is not blowing, and the sun is not always shining. Additionally, waves have the highest density of power compared to the other resources. The development of wave energy converters (WECs) aims to capture and convert it into carbon-free electricity [1]. Oscillating Wave Surge Converters (OWSCs) are the most popular type of the several WEC devices invented to capture the wave power [2]. OWSC is a bottom-hinged buoyant flap with a small thickness compared to the other dimensions. The relative rotational displacement between flap and base is converted into the electric power through a hydraulic power take-offs (PTO) system installed in the hinge. The PTO characteristic is modeled by a damping coefficient dissipating the wave energy, which, in turn, is added in the equation of the motion. They are designed to deploy in near-shore areas, where the shoaling effect and the horizontal acceleration of the water particles contribute to pivote pitching rotations around the hinge.

The hydrodynamics of flap as wave makers have been investigated by Dean and Dalrymple (1991) [3]. Later, Evans and Porter (1997) [4] studied the hydrodynamic characteristics of fully-submerged and surface-piercing flap plates. Renzi and Dias (2012) [5] have developed a 3D mathematical model in order to study the behavior of an OWSC in a channel. Assuming the inviscid and incompressible flow and linearizing the governing equations, the velocity potential in the fluid domain was obtained. The hydrodynamics of a single OWSC in the open ocean was studied by Renzi and Dias (2013) [6]. They introduced a semi-analytical model with small amplitude waves and inviscid, incompressible flow assumptions in the regular sea. The first full-scale surface piercing OWEC known as Oyster was successfully installed in Orkney Scotland in 2009 [7]. The mathematical framework describing the

hydrodynamics of Oyster has been given by a semi-analytical approach in [7]. In a numerical study by *Gomes et al*. (2015) [8], the hydrodynamics of a bottom-hinged flap that could be surface-piercing or fully submerged were investigated. Assuming linear hydrodynamic forces, they performed a parametric analysis in the frequency domain to approximate the extracted power for multiple plates with different geometries. It was shown that splitting a flap-type WEC into several vertical modules could result in improvements in power generation in addition to the reduction in foundation loading [9]. Physical modeling of a modular flap in a wave tank was performed in a model-scaled experiment by Wilkinson *et al*. (2017) [10] in a wide range of wave conditions. A comparison was made between the power captured from a single flap with that of a modular flap with the same total width. It was shown that the power generated by individual modules was not the same. Senol and Raessi (2019) [11] have proposed a technique for optimization of the power take-off system to improve power extraction. In this approach, both the linear and non-linear dynamics of the flap were taken into consideration. Saeidtehrani (2021) [12] has utilized a hybrid experimental-numerical approach to capture the non-linear dynamic of the array of flap-type WECs' behavior. Tongphong *et al*. (2021)[13] have investigated the capture factor of a floating modular flap, and four rafts hinged at the main floating structure have been experimentally investigated. It was shown that the wave frequency, PTO damping coefficient, considerably affected the WEC capture factor.

As mentioned in the previous studies, splitting a single plate into modules was shown to be effective. However, a mathematical study showing the effect of splitting a flap on the total induced power frequency response had not been investigated. A comparison between the performance of a single plate with that of a divided plate with the same total width is required. For this reason, in the present research work, a boundary element-based code and the MATLAB software are used to compare a single flap's power frequency response with ones for the equivalent double flap. The total projected surface is the same for single and double flap cases.

Therefore, this work is categorized as follows.

First, the theoretical background behind the mathematical modeling of OSWEC and the related governing dynamic equations is introduced. Secondly, the validation and correctness of the used approach are confirmed for a single flap compared to the previously published studies. Thirdly, the results of the double flaps are compared with the single one, and a comprehensive discussion is presented.

2. Theory

2.1. Dynamic governing equations

A bottom-hinged single flap-type OSWEC (SF-OSWEC) has a dynamic motion similar to a single degree of freedom inverted pendulum, which is affected by wave excitation forces. It is driven by the ocean waves, and is allowed to oscillate in the pitch mode around the horizontal axis at the hinge. The geometry of a rectangular flap with width W, height L, and thickness t in the Cartesian coordinate is shown in figure 1. As shown in the figure, the flap is hinged upon a foundation with a height of c. Considering a constant water depth h, under the action of the incoming monochromatic waves, the flap rotates with pitching amplitude $\theta(t)$, being zero when the plate is perpendicular to the sea bed. The x-axis is positive along the width of the flap, y is the direction of the propagating wave, and z is positive upward from the water surface.

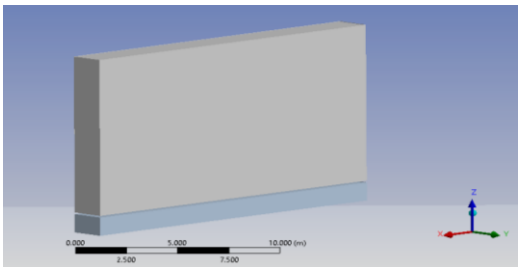

Figure 1. Geometry of a bottom-hinged flap.

Based on the Newton's second law, the dynamic governing motion of an SF-OSWEC is written as equation 1 exposed to the radiation $T_{rad}(t)$ and wave excitation diffraction and Froud Krylov torques called $T_{diff}(t)$ *and* $T_{F-K}(t)$.

$$\mathbf{I\ddot{\theta} = T_{diff}(t) + T_{F-K}(t) + T_{rad}(t) + T_{Pto}(t) + T_{hst}(t)} \quad (1)$$

where I is the mass moment inertia of the single flap, and $\ddot{\theta}$ is the acceleration of rotation. T_{rad} can be considered as the sum of two terms in phase with acceleration and velocity. T_{pto} is due to equivalent rotational damping of PTO, which can be introduced as $B_{pto}\dot{\theta}$. Hence, the corresponding equation for SF-OSWEC is as similar to the Cummins equation [14] in the time domain as follows:

$$\mathbf{(I + I_a(\infty))\ddot{\theta} + \int_{-\infty}^{t} K(t-\tau)\,\dot{\theta}(\tau)d\tau + B_{PTO}\dot{\theta}(t) + c\theta = T_{diff}(t) + T_{F-K}(t) = T_{ex}(t)} \quad (2)$$

In equation 2, I_a is added moment of inertia, B is the radiation damping, B_pto is the PTO damping, and C is the hydrostatic restoring coefficient. K is the impulse response function of the radiation.
On the other hand, the dynamic equations for double flap-type OSWEC (DF-OSWEC) can be presented in two independent equations by neglecting the interaction effects of separated flaps on each other. Therefore, the relation between the effective parameters is expressed as equation 3.

$$\begin{aligned}&(\mathbf{I_1}+\mathbf{I_{a1}}(\infty))\ddot{\boldsymbol{\theta}}_{\mathbf{1}}(\mathbf{t})+\int_{-\infty}^{\mathbf{t}}\mathbf{K_1}(\mathbf{t}-\boldsymbol{\tau})\,\dot{\boldsymbol{\theta}}_{\mathbf{1}}(\boldsymbol{\tau})\mathbf{d\tau}+\\&\mathbf{B_{PTO1}}\dot{\boldsymbol{\theta}}_{\mathbf{1}}(\mathbf{t})+\mathbf{C_1}\boldsymbol{\theta}_{\mathbf{1}}(\mathbf{t})=\mathbf{T_{1\_ex}}(\mathbf{t})\\&(\mathbf{I_2}+\mathbf{I_{a2}}(\infty))\ddot{\boldsymbol{\theta}}_{\mathbf{2}}(\mathbf{t})+\int_{-\infty}^{\mathbf{t}}\mathbf{K_2}(\mathbf{t}-\boldsymbol{\tau})\,\dot{\boldsymbol{\theta}}_{\mathbf{2}}(\boldsymbol{\tau})\mathbf{d\tau}+\\&\mathbf{B_{PTO2}}\dot{\boldsymbol{\theta}}_{\mathbf{2}}(\mathbf{t})+\mathbf{C_2}\boldsymbol{\theta}_{\mathbf{2}}(\mathbf{t})=\mathbf{T_{2\_ex}}(\mathbf{t})\end{aligned}\tag{3}$$

Assuming the harmonic behavior of the incident, diffraction, and radiation waves, the flap is set into a small-amplitude motion. The relationship between flap rotation in the time domain and complex amplitude of rotation Θ in the frequency domain can be written as equation 4:

$$\boldsymbol{\theta}(\mathbf{t})=\boldsymbol{\Theta}\mathbf{e}^{-\mathbf{i}\boldsymbol{\omega}\mathbf{t}}\tag{4}$$

Similarly, the excitation torque is expressed as:

$$\mathbf{T_{ex}}=|\mathbf{T_{ex}}|\mathbf{e}^{-\mathbf{i}\boldsymbol{\omega}\mathbf{t}}\tag{5}$$

Under an airy regular wave regime and linear PTO system, one can write the damped harmonic oscillation of a single and double configuration through the frequency domain analysis as:

$$\left[\boldsymbol{\omega}^{\mathbf{2}}(\mathbf{I}+\mathbf{I_a})-\mathbf{i}\boldsymbol{\omega}\left(\mathbf{B}+\mathbf{B_{pto}}\right)+\mathbf{C}\right]\boldsymbol{\Theta}=|\mathbf{T_{ex}}|\tag{6}$$

In equation 6, the added moment of inertia I_a, and radiation damping B are frequency-dependent. The PTO damping B_{pto} is assumed to be designed such that the maximum power is captured at every wave frequency. In the same procedure, the governing equations for double flap with two degrees of freedom is expressed as equation 7 in the frequency domain:

$$\begin{aligned}&-\boldsymbol{\omega}^{\mathbf{2}}\boldsymbol{\Theta}_{\mathbf{1}}(\mathbf{I_1}+\mathbf{I_{a1}})+\mathbf{i}\boldsymbol{\omega}\left(\mathbf{B_1}+\mathbf{B_{1_{PTO}}}\right)\boldsymbol{\Theta}_{\mathbf{1}}=|\mathbf{T_{1\_ex}}\\&-\boldsymbol{\omega}^{\mathbf{2}}\boldsymbol{\Theta}_{\mathbf{2}}(\mathbf{I_2}+\mathbf{I_{a2}})+\mathbf{i}\boldsymbol{\omega}\left(\mathbf{B_2}+\mathbf{B_{2_{PTO}}}\right)\boldsymbol{\Theta}_{\mathbf{2}}=|\mathbf{T_{2\_ex}}|\end{aligned}\tag{7}$$

More explanation is given in the following section. The coefficients of the added moment of inertia, radiation damping, and exciting Froud-Krylov and diffraction wave torque are frequency-dependent. These parameters cannot be calculated correctly via the analytical approach, and other methods such as the computational fluid dynamics and boundary element methods are utilized to calculate them. In the present work, the ANSYS-AQWA software based on the potential flow theory and solution method of the boundary element is used for computing the mentioned parameters. A brief description of the theory of the potential flow theory is presented in the following section. It can be noted that after calculating the hydrodynamic coefficients and excitation torques, solving the governing equation is conducted in the MATLAB software.
Considering a rectangular plate and assuming uniform mass distribution, the hydrostatic restoring coefficient C can be approximated by [8]:

$$\mathbf{C_{hydrostatic}}=\frac{(\mathbf{1}-\boldsymbol{\alpha})}{\mathbf{2}}\boldsymbol{\rho}_{\mathbf{w}}\mathbf{gtWL^2}\tag{8}$$

where α is the ratio of plate density ρ_p to water density, ρ_w g is the acceleration gravity, t is plate thickness, W is the plate width, and L is the plate height. It is noted that the viscous damping effects are neglected in this research work. It matches with a condition in which the induced vortex shedding decreases by removing the flap's sharp edges. Moreover, there is a limitation to using the above-mentioned equations near resonance because the large amplitude of the rotational displacement disrupts the linearized approximation of the formulas [8]. Hence the results obtained are plotted before resonance in the present work.

2.2. Potential flow theory

The Navier-Stokes equations should be solved in order to derive the hydrodynamic coefficients and wave excitation torque. However, as the water density ρ is not expected to have significant changes in wave-body interactions, the fluid is considered incompressible. Additionally, the wave amplitude A is much smaller than the characteristic width W. The fluid can be considered inviscid and irrotational within this assumption, as in the potential flow theory. Hence, a velocity potential exists, and conservation of mass satisfies the governing Laplace equation.

$$\boldsymbol{\nabla}^{\mathbf{2}}=\mathbf{0}\tag{9}$$

The physical expression of oscillating water waves describes the generated waves of fluid-structure interaction at frequency ω yields:

$$\boldsymbol{\Phi}=\mathbb{R}\{(\boldsymbol{\phi_I}+\boldsymbol{\phi_R}+\boldsymbol{\phi_D})\boldsymbol{e}^{-\boldsymbol{i\omega t}}\}\tag{10}$$

Equation 10 represents the solution to the boundary value problem. ϕ_I is the incident wave potential function, ϕ_D represents the diffracted

wave potential function in the presence of the fixed flap, and ϕ_R is the radiation wave field generated due to flap oscillations. The hydrodynamic coefficients are computed regarding the radiation potential, while ϕ_I and ϕ_D create the exciting torques on the flap.

2.3. Power frequency response

The complex amplitude of the flap rotation in the frequency domain can be obtained by solving equation 6 The frequency-dependent complex amplitude of flap rotation can be written as [8]:

$$\Theta(\omega) = \frac{|T_{ex}|}{[\omega^2(I+I_a) - i\omega(B+B_{pto}) + C]} \quad (11)$$

Since the methodology is based on the linear wave theory, the response amplitudes larger than 30° should not be considered based on the assumption of small-amplitude waves [8]. Assuming linear PTO, the average power extracted over a cycle of rotation can be written as [15]:

$$P(\omega) = \frac{1}{2}\omega^2 B_{pto} |\Theta(\omega)|^2 \quad (12)$$

2.4. Optimum damping

The damping factor of the PTO system is an effective parameter of the total output power. It can be observed that the output power is dependent on the damping and rotational amplitude of the flap. As shown in equation 12 an increase in damping can directly enhance the harvested energy from the vibrations of the oscillating flap. On the other hand, damping rise reduces the rotational displacement, decreasing the output power. Therefore, an optimum damping value contributes to the maximum output power. Since the output power function in equation 12 is an analytical expression versus the damping, for a linear system, the optimum PTO damping can be derived as [15]:

$$B_{pto-opt} = \sqrt{B^2 + (\frac{C}{\omega} - \omega(I + I_a))^2} \quad (13)$$

It is demonstrated that the same formula can be utilized for each one of the flaps in the double configuration because each flap's equation of motion is independent. The optimum damping given in equation 13 is the frequency-dependent parameter that should be tuned for each sea-state. In the real conditions, this is done by a control system.

3. Validation

The crucial point regarding solving the governing equation is computing the frequency-dependent parameters of the added moment of inertia, radiation damping, and wave exciting torque. In order to validate the hydrodynamic coefficients in the frequency domain, a comparison is made between the values obtained from the semi-analytical approach by Renzi and Dias (2013)[6] and the numerical results with ANSYS AQWA. The characteristic values of the flap and considered regular waves are shown in Table 1.

Table 1. Characteristics of single flap for numerical model.

Flap width (m)	**18**
Foundation height (m)	1.5
Water depth (m)	10.9
Incident wave amplitude (m)	0.3
Mass (kg)	61216
Moment of inertia ($kg.m^2$)	1.80e6
Center of gravity to hinge (m)	4.7

Figures 2, 3, and 4 show the plots of the added moment of inertia, damping, and exciting torque as the functions of the period. It is observed that the resulting hydrodynamic coefficients and exciting torques obtained by the boundary element method in AQWA are approximately in good agreement with the study by Renzi and Dias (2013) [6].

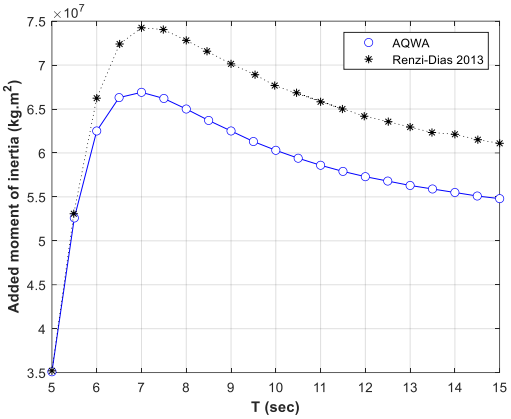

Figure 2. Added moment of inertia coefficient.

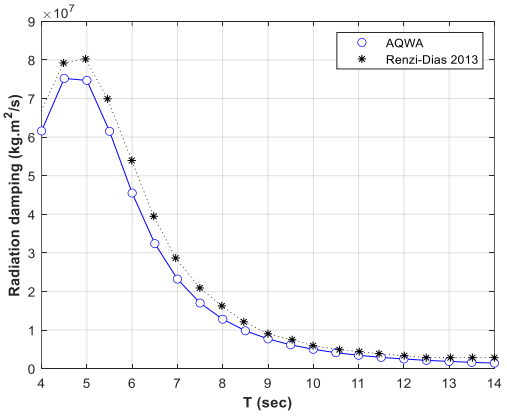

Figure 3 Radiation damping coefficient.

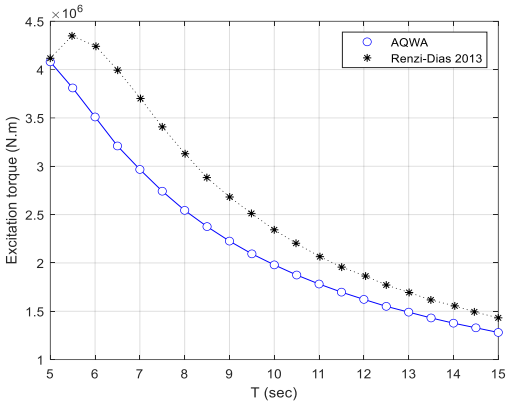

Figure 4. Excitation torque.

As it can be seen, there is a difference between the hydrodynamic coefficients obtained from AQWA and the semi-analytical model, though the flap width and the water depth are the same. This difference may be attributed to the modeling conditions. In the AQWA model, the flap is modeled submerged but in the model by Renzi-Dias, the plate is surface-piercing.

4. Results and Discussion

In the validation section, the correctness of the simulating procedure has been confirmed for a single flap. A similar method is used for deriving the corresponding parameters of each one of the double-separated flaps. The geometry of the double flap is shown in figure 5. Each flap has the same height and thickness as the single flap. A foundation with the same geometry is also included. The width for each flap is 9 m, half of the single one.

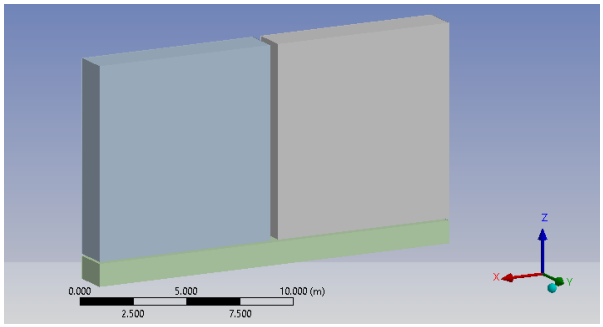

Figure 5. Geometry of a double flap.

Figures 6, 7, and 8 show the variation of hydrodynamic coefficients and torques for each flap in the double configuration *vs.* single. These parameters are dependent on the geometry and the surface area interacting with water. As shown in figure 8 the smaller surface area of each flap in the double configuration induces lower wave radiation torques than the single one. Consequently, decomposing the radiation torques in two separate terms, in phase with rotational acceleration and velocity, causes lower rotational damping and added moment of inertia coefficients than the single one, as observed in figures 6 and 7. Similarly, the excitation torque including the Froud-Krylov and diffraction terms decreases for each plate of the double arrangement compared to a single one.

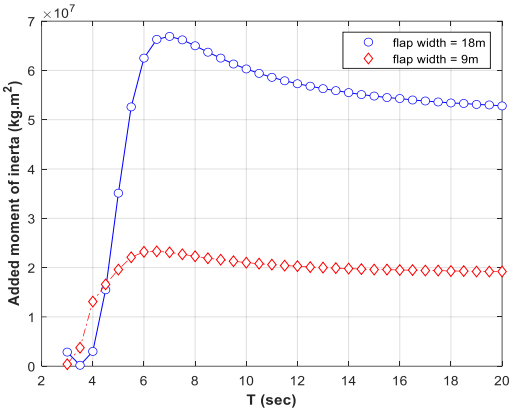

Figure 6. Added moment of inertia coefficient for single and double configuration.

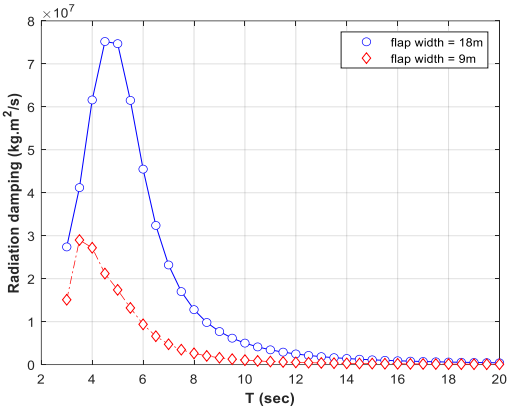

Figure 7. Radiation damping coefficient for single and double configuration.

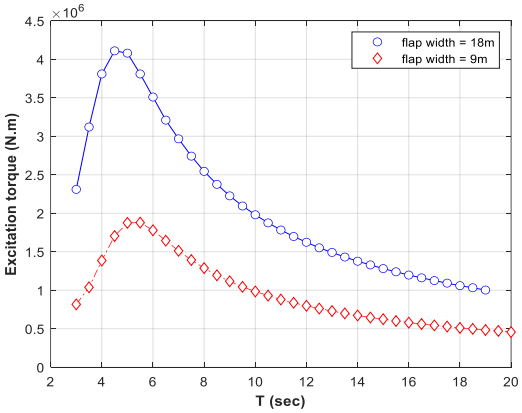

Figure 8. Excitation torque applied on single flap and each plate of double configuration.

Altering the plate's dimension from single to double configuration causes the dynamic parameters such as the mass moment of inertia

and hydrostatic stiffness to be changed. Therefore, the natural frequency of the system is expected to be modified. It will be shown that this modification can be advantageous in capturing the total power from the incident waves. It is worth mentioning that, in this work, the interactions between the flaps are not considered.

The rotational displacement of the single and double configuration is shown in figure 9. It is demonstrated that after the wave period $T \approx 4.3\ s$, the pitch rotation for each one of the double flaps becomes larger than that of the single flap. Additionally, as the resonance period of the divided flaps is lower than that of the single, the angle of rotation in double plates increases at a higher rate than the single plate.

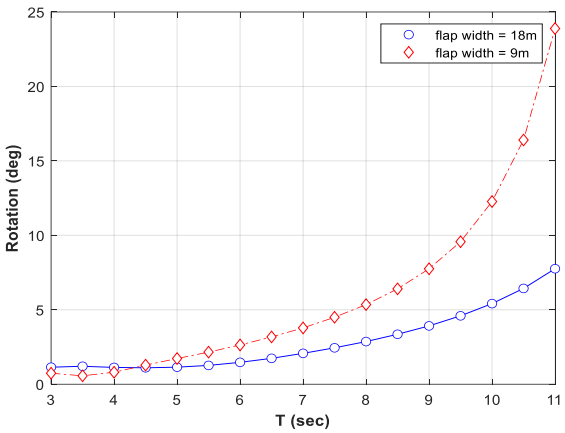

Figure 9. Amplitude of rotational displacement for single and double configurations.

One of the crucial aims of this work was to find the power change versus the excitation period in the single and double arrangement.

The total extracted power with respect to the incoming wave period is plotted in figure 10. As it can be seen, at thye wave periods greater than $4.5\ s$, the total extracted PTO power from the double flap is higher than that of the single flap. This improvement in power extraction is due to the modifications in the dynamic properties of the system after splitting the single flap into two plates. The natural period of the flap is directly dependent on $I + I_a$, while it inversely changes with C, as in equation 14.

$$\mathbf{T_n = 2\pi\sqrt{\frac{I+I_a}{C}}} \qquad (14)$$

The mass moment of inertia and rotational hydrostatic stiffness values for each double case flap is reduced to half of the single ones. However, the reduction of I_a is more considerable, and it decreases below the half of one related to the single flap. Therefore, the natural period of each flap is a smaller value than for a single flap. This causes the peak in the curve of power versus the period to move close to the origin, and consequently, higher values of the total power are observed at the small wave excitation periods for double configuration compared to the single one.

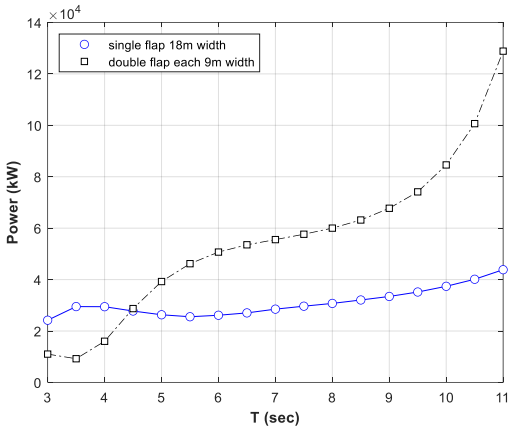

Figure 10. Total power extracted from single and double configurations.

The wave period is a major variable in the response of a wave energy converter [16], and the range of periods shown in figure 10 corresponds to the response obtained by a linear assumption. From this result obtained in the frequency domain, it can be deduced that splitting a single plate can enhance power extraction in the typical range of wave periods in the nearshore area.

It is noted that although the power depends on the amplitude of the rotational displacement, the peak period of the power and displacement do not match each other. The reason is related to the fact that the rotational displacement is also dependent on the wave period.

5. Conclusion

In the present work, the effect of splitting a single flap into a double arrangement on the total extracted power was investigated numerically, while the total wet surface area of the plates remained constant for both configurations. A boundary element method code was utilized for deriving the hydrodynamic coefficients and exciting torques, while the governing equations were solved via the MATLAB software. The results obtained confirmed that the dynamic properties of the small separated flaps induced a lower natural period than those for a single larger flap. This consequently resulted in a wideband response of the output extracted power for the double case at a wider range of low excitation periods when compared to a single flap. Additionally, it could be concluded from the

results that in the range of wave periods corresponding to linear oscillations, the pitch rotations in divided flaps were larger than that of the single. As the average power is proportional to the square of absolute of the rotation, the total power extraction can be enhanced after splitting the flap with the configuration shown in this work.

6. References

[1] A. F. d. O. Falcão, "Wave energy utilization: A review of the technologies," Renew. Sustain. Energy Rev., Vol. 14, No. 3, pp. 899–918, 2010, doi: 10.1016/j.rser.2009.11.003.

[2] A. Babarit, "A database of capture width ratio of wave energy converters," Renew. Energy, Vol. 80, pp. 610–628, 2015, doi: 10.1016/j.renene.2015.02.049.

[3] R. G. Dean and R. A. Dalrymple, Water wave mechanics for engineers and scientists. 1991.

[4] D. V. Evans and R. Porter, "Efficient calculation of hydrodynamic properties of owc-type devices," J. Offshore Mech. Arct. Eng., Vol. 119, No. 4, pp. 210–218, 1997, doi: 10.1115/1.2829098.

[5] E. Renzi and F. Dias, "Resonant behaviour of an oscillating wave energy converter in a channel," J. Fluid Mech., Vol. 701, No. June, pp. 482–510, 2012, doi: 10.1017/jfm.2012.194.

[6] E. Renzi and F. Dias, "Hydrodynamics of the oscillating wave surge converter in the open ocean," Eur. J. Mech. B/Fluids, Vol. 41, pp. 1–10, 2013, doi: 10.1016/j.euromechflu.2013.01.007.

[7] E. Renzi, K. Doherty, A. Henry, and F. Dias, "How does Oyster work? the simple interpretation of Oyster mathematics," Eur. J. Mech. B/Fluids, Vol. 47, No. June 2012, pp. 124–131, 2014, doi: 10.1016/j.euromechflu.2014.03.007.

[8] R. P. F. Gomes, M. F. P. Lopes, J. C. C. Henriques, L. M. C. Gato, and A. F. O. Falcão, "The dynamics and power extraction of bottom-hinged plate wave energy converters in regular and irregular waves," Ocean Eng., Vol. 96, pp. 86–99, 2015, doi: 10.1016/j.oceaneng.2014.12.024.

[9] L. Wilkinson, K. Doherty, J. Nicholson, T. Whittaker, and S. Day, "Modelling the Performance of a Modular Flap-Type Wave Energy Converter," in 11th European Wave and Tidal Energy Conference, 2015, No. November.

[10] L. Wilkinson, T. J. Whittake, P. Thies, A. Day, and D. Ingram, "The power-capture of a nearshore, modular, flap-type wave energy convertor in regular waves," Ocean Eng., Vol. 137, pp. 394–403, 2017.

[11] K. Senol and M. Raessi, "Enhancing power extraction in bottom-hinged flap-type wave energy converters through advanced power take-off techniques," Ocean Eng., Vol. 182, no. December 2018, pp. 248–258, 2019, doi: 10.1016/j.oceaneng.2019.04.067.

[12] S. Saeidtehrani, "Flap-type wave energy converter arrays : Nonlinear dynamic analysis," Ocean Eng., Vol. 236, No. October 2020, p. 109463, 2021, doi: 10.1016/j.oceaneng.2021.109463.

[13] W. Tongphong, B. Kim, I. Kim, and Y. Lee, "A study on the design and performance of ModuleRaft wave energy converter," Renew. Energy, Vol. 163, pp. 649–673, 2021, doi: 10.1016/j.renene.2020.08.130.

[14] W. E. Cummins, "The impulse response function and ship motion," 1962.

[15] J. Falnes, Ocean Waves and Oscillating Systems. Cambridge University, 2002.

[16] T. Whittaker and M. Folley, "Nearshore oscillating wave surge converters and the development of Oyster," Philos. Trans. R. Soc. A Math. Phys. Eng. Sci., Vol. 370, No. 1959, pp. 345–364, 2012, doi: 10.1098/rsta.2011.0152.